Int. Conf. on Pattern Recognition, Vienna, Autria, august 1996

STATISTICAL MODEL-BASED ESTIMATION AND TRACKING OF NON-RIGID MOTION

C. Kervrann†, F. Heitz‡ & P. Pérez†

† IRISA/INRIA Rennes - Université de Rennes I
Campus universitaire de Beaulieu - 35042 Rennes Cedex, France
{kervrann,perez}@irisa.fr

‡ ENSPS/LSIIT, URA CNRS 1871,
Boulevard Sébastien Brant, 67400 Illkirch, France.
heitzfa@enspsmail.u-strasbg.fr

Abstract

We describe a method for the temporal tracking of stochastic deformable models in image sequences. The object representation relies on a hierarchical statistical description of the deformations applied to a template. The optimal bayesian estimate of deformations is obtained by maximizing non-linear probability distributions using optimization techniques. The method may be sensitive to local maxima of the distributions and require an initial configuration close to the optimal solution. In our approach, the initialization is provided by a robust estimate of the rigid and statistically constrained non-rigid motions from the normal optical flow computed along the deformable contour. The approach is demonstrated on real-world sequences showing mouth movements and cardiac motions with missing data.

1 Introduction

Tracking algorithms have been recently performed to determine 2D motion and deformations of complex shapes in image sequences. The representation and processing of deformations has many potential applications, for instance in biomedical image analysis [7, 16] or in human-computer interaction [5, 20, 10]. Deformable models have been introduced to incorporate geometric information about shapes and their variations and motion [5, 16]. Active contour models attempt to extract regions of interest throughout the sequence and accurately delineate the shapes by applying an image force field that is computed from the gradient of the intensity image [11, 20, 16]. Additional *a priori* constraints have been imposed to improve the initial location of deformable structures and to control the deformable contour displacements during the optimization process. Previous works combine stochastic filtering (Kalman filter) and optimization of the deformable contour points under an affine motion constraint [5, 1] or propose a modal analysis of the physical motion of the dynamic contour [9]. An alternative approach consists in using a dense optical flow field to displace the deformable contour points [7] ; in some cases, the information given by optical flow measurements computed along the deformable contour only is required to constrain the deformable contour optimization accordingly [3]. Another class of approach addresses the problem of tracking a region surrounding the feature of interest [1, 4]. Affine motion models provide greater abstraction and robustness than the purely flow-based methods yet are weaker if models do not incorporate detailed information about shape [1, 14].

In [12], we have introduced a hierarchical statistical deformable model able to constrain the *a priori* structure and the global and local shape deformations. In this approach, local deformations modeled as local stochastic perturbations and the Karhunen Loeve (KL) analysis allow to approximate the global deformations observed on a training set of representative shapes [8]. A *Marginalized Maximum Likelihood* (MML) estimate of the global deformations and a Maximum A Posterori (MAP) estimate of the deformable template are finally derived by maximizing probability distributions describing the interactions between observations and the unknown variables. This general framework is reported in section 2.

When the shape of the target feature is approximatively known, it is desirable to incorporate a strong tendency to a particular initial configuration of the model in each frame [5, 13]. Incorporating knowledge on the motion reduces the model to be distracted when the tracked structure moves over background clutter and solve the problem of the initialization of the model before the deterministic optimization process is performed. Here, this is achieved by coupling a normal optical flow field to a statistical deformable template. The rigid and non-rigid parametric motions are estimated over an image sequence using a robust regression scheme from optical flow measurements computed along the deformable contours. This approach is described in section 3 and provides initial estimates of the deformation process. The approach is able to cope with large motion magnitudes and enables to track reliably deformable structures on real-world image sequences showing mouth movements and cardiac motions (section 5).

2 Stochastic deformable model-based segmentation

In this section, we present a general framework for segmentation which relies on a bayesian estimation scheme incorporating the *a priori* deformable model.

2.1 A stochastic shape model

The approach described in [12] relies on the description of the object class of interest using a "deformable template" which incorporates *a priori* knowledge on the structure of the object and its variability [8]. A particular shape $\mathbf{x}$ is represented by a set of n labeled points which approximate its outline. The variations of shape $\mathbf{x}$ are represented by a displacement vector $\mathbf{dx} = \mathbf{x} - \bar{\mathbf{x}}$ with respect to a mean shape (the "template") $\bar{\mathbf{x}}$ [8]. A Principal Component Analysis (PCA) on the displacement vectors computed from the set of training shapes allows to determine the m most significant deformation modes. If $\mathbf{\Phi} = [\,\phi_{x_1}, \phi_{y_1}, \cdots, \phi_{x_n}, \phi_{y_n}\,]^T$ designates the $(2n \times m)$ matrix of the m unit eigenvectors corresponding to the m largest eigenvalues, and if $\mathbf{b}$ denotes the modal amplitudes vector $(m \times 1)$ corresponding to the m deformation modes, the deformable template is represented by the following model [12]:

$$\mathbf{X} \;=\; \mathbf{M}(k,\theta)\;[\,\bar{\mathbf{x}} \;+\; \mathbf{\Phi}\,\mathbf{b}\,] \;+\; \mathbf{T}. \qquad (1)$$

From Eq. 1, a shape in the model frame is transformed into the image frame by a $2n \times 1$ translation vector $\mathbf{T} = [T_x,\, T_y,\, \cdots]^T$ and by a $2n \times 2n$ rotation of angle θ and scaling by factor k matrix $\mathbf{M}(k,\theta) = diag(M(k,\theta))$ with :

$$M(k,\theta) = \begin{bmatrix} \varsigma & -\upsilon \\ \upsilon & \varsigma \end{bmatrix} = \begin{bmatrix} k\cos\theta & -k\sin\theta \\ k\sin\theta & k\cos\theta \end{bmatrix}. \qquad (2)$$

In this modeling, let point out that the matrix of m unit eigenvectors $\mathbf{\Phi}$ and the mean vector $\bar{\mathbf{x}}$ are definitively estimated *off-line*.

A local deformation process is introduced to refine this first (eventually crude) description. Local deformations $\boldsymbol{\delta}$ are modeled as random perturbations on the location of the points belonging to the globally deformed pattern and are assumed to follow a first-order zero-mean Gauss-Markov random process :

$$\mathsf{P}\,(\,\boldsymbol{\delta}\,) \;=\; \frac{1}{Z_p}\;\exp -\frac{1}{2}\;\boldsymbol{\delta}^T\;\mathbf{R}^{-1}\,\boldsymbol{\delta} \qquad (3)$$

where $\mathbf{R}$ is the covariance matrix of $\boldsymbol{\delta}$ and Z_p is the partition function. The complete parametric deformable model (denoted $\mathbf{Y}$) becomes :

$$\mathbf{Y} \;=\; \mathbf{M}(k,\theta)\;[\,\bar{\mathbf{x}} \;+\; \mathbf{\Phi}\,\mathbf{b}\,] \;+\; \mathbf{T} \;+\; \boldsymbol{\delta}. \qquad (4)$$

2.2 Bayesian estimation of deformations

The stochastic deformable model is used to extract moving objects from image sequences. The MAP estimate of the deformable template is defined by:

$$\mathbf{Y}^* \;\stackrel{\triangle}{=}\; \arg\max_{\mathbf{Y}}\; \mathsf{P}\,(\mathbf{d}\,|\,\mathbf{Y})\;\mathsf{P}\,(\mathbf{Y}). \qquad (5)$$

The prior distribution of $\mathbf{Y}$ is a Gauss-Markov distribution according to the assumption on the statistics of $\boldsymbol{\delta}$ (Eq. 3). A (gibbs) distribution $\mathsf{P}(\mathbf{d}\,|\,\mathbf{Y})$ describes the interactions between the observations $\mathbf{d}$ and the deformations to estimate :

$$\mathsf{P}\,(\mathbf{d}\,|\,\mathbf{Y}) \;\propto\; \exp -E_d(\mathbf{Y},\mathbf{d}) = \exp \sum_{s\,\in\,\Gamma_{\mathbf{Y}}} \|\vec{\nabla} I_s\| \qquad (6)$$

where $E_d(\mathbf{Y},\mathbf{d})$ is an energy function which tends to attract the contour of the deformable template $\Gamma_{\mathbf{Y}}$ toward salient features of the image corresponding to large spatial gradients, denoted $\|\vec{\nabla} I_s\|$ at site s in the image [11, 13]. The MAP estimate of deformations may be expressed as:

$$\mathbf{Y}^* \;=\; \arg\max_{\mathbf{Y}}\; \frac{1}{Z}\;\exp\;\; - E_{\mathbf{\Theta}}(\mathbf{Y},\mathbf{d}) \qquad (7)$$

where the joint distribution $\mathsf{P}\,(\mathbf{Y},\mathbf{d}\,|\,\mathbf{\Theta})$ has been rewritten as a Gibbs distribution, $\mathbf{\Theta} \;=\; [\,\mathbf{M}(k,\theta),\, \mathbf{T},\, \mathbf{b}\,]$ is the hidden *hyperparameter* vector of the probabilistic model $\mathbf{Y}$ (the partition function Z does not depend on $\mathbf{\Theta}$) and $E_{\mathbf{\Theta}}(\mathbf{Y},\mathbf{d})$ is an energy function :

$$E_{\mathbf{\Theta}}(\mathbf{Y},\mathbf{d}) \;=\; -\sum_{s\,\in\,\Gamma_{\mathbf{Y}}} \|\vec{\nabla} I_s\| \;+\; \frac{1}{2}(\mathbf{Y}-\mathbf{X}(\mathbf{\Theta}))^T\mathbf{R}^{-1}(\mathbf{Y}-\mathbf{X}(\mathbf{\Theta})). \qquad (8)$$

2.3 Marginalized Maximum Likelihood

Since $\mathbf{\Theta}$ is unknown, the problem of estimating the pair $(\widehat{\mathbf{\Theta}}, \widehat{\mathbf{Y}})$ according to the above criterion (7) of optimality remains extremely difficult to implement in practice. The idea we propose is to consider the hidden hyperparameters $\mathbf{\Theta}$ at a different level than $\mathbf{Y}$. Thus, $\mathbf{\Theta}$ may be estimated by marginalizing with respect to $\mathbf{Y}$ [15] :

$$\mathbf{\Theta}^* = \arg\max_{\mathbf{\Theta}} \int_{\mathbf{Y}} \mathsf{P}(\mathbf{Y}, \mathbf{d} \,|\, \mathbf{\Theta})\, d\mathbf{Y} \tag{9}$$

Under the assumption that $\mathbf{Y}$ is very concentrated around $\mathbf{X}(\mathbf{\Theta})$, we have :

$$\mathsf{P}(\mathbf{Y} \,|\, \mathbf{\Theta}) \approx \delta(\mathbf{Y} - \mathbf{X}(\mathbf{\Theta})) \tag{10}$$

where $\delta(\cdot)$ designates the Dirac function. We obtain:

$$\begin{aligned} \mathbf{\Theta}^* &= \arg\max_{\mathbf{\Theta}} \int_{\mathbf{Y}} \mathsf{P}(\mathbf{d} \,|\, \mathbf{Y}, \mathbf{\Theta})\, \delta(\mathbf{Y} - \mathbf{X}(\mathbf{\Theta}))\, d\mathbf{Y} \\ &= \arg\max_{\mathbf{\Theta}} \mathsf{P}(\mathbf{d} \,|\, \mathbf{Y} = \mathbf{X}(\mathbf{\Theta})) \end{aligned} \tag{11}$$

and from Eq. 8 the estimate of $\mathbf{\Theta}$ is finally given by:

$$\mathbf{\Theta}^* = \arg\min_{\mathbf{\Theta}} E_d(\mathbf{X}(\mathbf{\Theta}), \mathbf{d}). \tag{12}$$

Finally, the MAP estimate of $\mathbf{Y}$ is easily derived given the optimal estimate $\mathbf{\Theta}^*$ where the criterion is equivalent to minimize a global energy function:

$$\mathbf{Y}^* = \arg\min_{\mathbf{Y}} E_{\mathbf{\Theta}^*}(\mathbf{Y}, \mathbf{d}). \tag{13}$$

In practice, the estimation of $\mathbf{\Theta}$ and $\mathbf{Y}$ are performed using a steepest descent gradient algorithm in all experiments.

3 Robust Estimation of non-rigid motions

We take advantage of the temporal coherence of the object movements to predict the location of the model in each image. If $\mathbf{X}_{t+1}$ is expanded in Taylor series to the first order at time $t+\delta t$, the corresponding dynamics of the global parameters are easily derived [13] :

$$\left\{ \begin{array}{lcccc} \mathbf{T}_{t+\delta t} & = & \mathbf{T}_t & + & \delta t\, \dot{\mathbf{T}}_t \\ \mathbf{M}_{t+\delta t} & = & \mathbf{M}_t & + & \delta t\, \dot{\mathbf{M}}_t \\ \mathbf{b}_{t+\delta t} & = & \mathbf{b}_t & + & \delta t\, \dot{\mathbf{b}}_t \end{array} \right.$$

where the first order temporal derivatives $\dot{\mathbf{T}}_t = [\dot{T}_x, \dot{T}_y, \cdots]^T$, $\dot{\mathbf{M}}_t = diag(\dot{M}_t)$ and $\dot{\mathbf{b}}_t$ express the velocities of the parameters $\mathbf{T}_t$, $\mathbf{M}_t$ and $\mathbf{b}_t$ respectively and δt is the time step between two successive frames. The dynamic information is given in our approach by a normal optical flow field computed along the deformable model contour. The model motion is then naturally decomposed into two rigid and non-rigid components and constrains the prediction in each frame of the sequence.

3.1 Temporal evolution of the deformable template

The determination of the parametric motion relies on the analysis of the dynamic behavior of the deformable template $\mathbf{X}$. The local deformation process is not considered here because of its sensitivity to spatio-temporal measurements. At time t, the first order temporal derivative $\dot{\mathbf{X}}_t = [\dot{X}_1^t, \cdots, \dot{X}_n^t]^T$ may be expressed as:

$$\dot{\mathbf{X}}_t = \dot{\mathbf{M}}_t\, [\bar{\mathbf{x}} + \mathbf{\Phi}\, \mathbf{b}_t] + \mathbf{M}_t\, \mathbf{\Phi}\, \dot{\mathbf{b}}_t + \dot{\mathbf{T}}_t. \tag{14}$$

and the matrix of the unit eigenvectors $\mathbf{\Phi}$ and the mean vector $\bar{\mathbf{x}}$ doe not depend on t. The first order derivative of any control point of the model $X_i^t = [X_{x_i}^t, X_{y_i}^t]^T$ is thus :

$$\begin{aligned} \begin{bmatrix} \dot{X}_{x_i}^t \\ \dot{X}_{y_i}^t \end{bmatrix} &= \begin{bmatrix} \dot{\varsigma}^t & -\dot{\upsilon}^t \\ \dot{\upsilon}^t & \dot{\varsigma}^t \end{bmatrix} \begin{bmatrix} \bar{x}_{x_i} + \boldsymbol{\phi}_{x_i} \mathbf{b}_t \\ \bar{x}_{y_i} + \boldsymbol{\phi}_{y_i} \mathbf{b}_t \end{bmatrix} \\ &+ \begin{bmatrix} \varsigma^t & -\upsilon^t \\ \upsilon^t & \varsigma^t \end{bmatrix} \begin{bmatrix} \boldsymbol{\phi}_{x_i} \dot{\mathbf{b}}_t \\ \boldsymbol{\phi}_{y_i} \dot{\mathbf{b}}_t \end{bmatrix} + \begin{bmatrix} \dot{T}_x^t \\ \dot{T}_y^t \end{bmatrix}. \end{aligned} \tag{15}$$

Defining $\mathbf{\Xi}$ as :

$$\mathbf{\Xi} = [\dot{\varsigma}^t,\, \dot{\upsilon}^t,\, \dot{T}_x^t,\, \dot{T}_y^t,\, \dot{\mathbf{b}}_t^T]^T. \tag{16}$$

where the four first parameters describe the rigid component of the motion and $\dot{\mathbf{b}}_t$ is referred as the deformable motion parameters, $\dot{X}_i^t = [\dot{X}_{x_i}^t, \dot{X}_{y_i}^t]^T$ can be stated in the following way:

$$\dot{X}_i^t = \mathbf{W}_i\, \mathbf{\Xi} \tag{17}$$

$$\mathbf{W}_i = \begin{bmatrix} \bar{x}_{x_i} + \boldsymbol{\phi}_{x_i} \mathbf{b}_t & -\bar{x}_{y_i} - \boldsymbol{\phi}_{y_i} \mathbf{b}_t & 1 & 0 & \varsigma^t \boldsymbol{\phi}_{x_i} - \upsilon^t \boldsymbol{\phi}_{y_i} \\ \bar{x}_{y_i} + \boldsymbol{\phi}_{y_i} \mathbf{b}_t & \bar{x}_{x_i} + \boldsymbol{\phi}_{x_i} \mathbf{b}_t & 0 & 1 & \upsilon^t \boldsymbol{\phi}_{x_i} + \varsigma^t \boldsymbol{\phi}_{y_i} \end{bmatrix}$$

which is linear with respect to the $(m+4)$ motion parameters $\mathbf{\Xi}$.

3.2 A statistical B-spline model

A shape is represented by a B-spline curve with its n control points $X_i^t = [X_{x_i}^t, X_{y_i}^t]^T$ corresponding to the "landmarks" defined in section 2. Such a B-spline based representation of curved edges is attractive because B-splines can describe most real-world shapes rather realistically [1, 2]. From a mathematical point of view, a B-spline curve is piecewise polynomial. As a

B-spline curve, $\mathtt{X}_t(u) = [\mathtt{x}_t(u),\, \mathtt{y}_t(u)]^T$ (with $u \in [1, n]$) can be written as a linear combination of the B-spline basis functions $\mathcal{B}(.)$ and control points X_i^t:

$$\mathtt{X}_t(u) = \begin{bmatrix} \mathtt{x}_t \\ \mathtt{y}_t \end{bmatrix} (u) \;=\; \sum_{i=1}^{n} \mathcal{B}_i(u)\, X_i^t. \qquad (18)$$

In our approach, the deformable B-spline curve is indeed parametrized by the global parameters $\boldsymbol{\Theta}$ and not by its shape control points as done classically. If $\dot{\mathtt{X}}_t(u) = [\dot{\mathtt{x}}_t(u),\, \dot{\mathtt{y}}_t(u)]^T$ denotes the first order temporal derivative of a point $\mathtt{X}_t(u)$ and the B-spline basis does not depend on t, we may write:

$$\dot{\mathtt{X}}_t(u) \;=\; \sum_{i=1}^{n} \mathcal{B}_i(u)\, \dot{X}_i^t \;=\; \sum_{i=1}^{n} \mathcal{B}_i(u)\, \mathbf{W}_i\, \Xi. \qquad (19)$$

3.3 Robust regression

We have computed normal displacements (denoted $\dot{\mathtt{X}}_t^{\perp}(u)$ hereafter at point $\mathtt{X}_t(u)$) along contours determined by the deformable contour in image sequences using the technique described in [6] ; it is well known that the so-called aperture problem restricts the estimation to the perpendicular-to-the-edge motion component only. The motion estimation technique under concern has the advantage to cope with large motion magnitudes and any class of contours that differential methods cannot handle properly.

The estimation of the motion parameters Ξ relies on the adjustment of the model to the corrupted measurements [19, 3]. If $\mathtt{n}(u) = [\mathtt{n}_x(u),\, \mathtt{n}_y(u)]^T$ denotes the unit normal to the deformable contour at point $\mathtt{X}_t(u)$, we have:

$$\dot{\mathtt{X}}_t^{\perp}(u) \;=\; \sum_{i=1}^{n} \mathcal{B}_i(u)\, \mathtt{n}^T(u)\, \mathbf{W}_i\, \Xi \;=\; A_i(u)\, \Xi. \qquad (20)$$

Although the object shape is represented by a continuous curve, it is convenient in practice to sample the curve with p points $\{u_i\}_{i=1}^{p}$.

In statistical analysis, the goal of robust estimation is to find the parameters Ξ which best fits a model $A_i(u)\ \Xi$ to the observations $\dot{\mathtt{X}}_t^{\perp}(u)$, when some data behave like outliers. Classical statistical robust estimators can tolerate up to $\frac{1}{k+1}\%$ outliers where k is the number of parameters of the model to estimate. The number of motion parameters is $k = m + 4$ and the breakdown point does not exceed 0.08 or 0.1 respectively if m corresponds to 5 to 7 deformation modes typically. So we prefer to adopt the least-median-of-squares (LMedS) estimator since it remains reliable up to 50% of the data as outliers. The parameters are estimated by solving the non linear minimization problem:

$$\widehat{\Xi} = \arg\min_{\Xi}\ \mathrm{Med}_{i\in[1,\cdots,p]} \left(\dot{\mathtt{X}}_t^{\perp}(u_i) - A_i(u_i)\, \Xi \right)^2. \quad (21)$$

The computation cost is not too high in our case because of the low amount of data on the one hand and the use of the speed-up technique described in [18] in the other hand. We use LMedS for its ability to detect outliers and a mean square solution is derived affer elimination of these outliers to cope with the inefficiency of LMedS in the case of Gaussian noise.

4 Experimental results

In our first experiments, we have considered the segmentation and tracking of a mouth. In this case, the model is initialized by hand intervention on the first frame, close to the optimal configuration [13]. The motion of the mouth estimated between two frames is used to predict automatically the location of the feature of interest in the subsequent frames. The different steps of the tracking procedure are demonstrated on two frames of a sequence composed of more than one hundred 128×128 frames (Fig.1). Fig.1a shows the result of the estimation of the normal flow field along the deformable B-spline contour at time t (15sec cpu time on Sun Sparc10). In this case the measurements are corrupted in the region of interest because of low contrast but contain some information corresponding to important displacement magnitudes of the non-rigid object. A robust regression is necessary to extract the useful dynamic information (4+7 parameters) to predict the location of the model in the next frame at time $t + \delta t$ (Fig 1c) and requires 1mn cpu time on Sun Sparc10. However, the prediction of the global parameters $\boldsymbol{\Theta}$ computed from the estimation of Ξ is rather inaccurate. So this result is considered as an initialization to the estimation of the global parameters $\boldsymbol{\Theta}$ and the local deformations $\boldsymbol{\delta}$, requiring 15sec on Sun Sparc10 (Fig.1e) . From the segmentation result given by the estimation of the global parameters, a new optical flow field is computed at time $t+\delta t$ along the deformable contour (fig.1b). The prediction of the model at time $t + 2\delta t$ and the final segmentation result are presented respectively in Fig.1d and Fig.1f.

The second experimental results allow to demonstrate the ability of the method to solve the problem of tracking of a cardiac left ventricle in X-ray imagery and in ultrasound imagery ; the final segmentation results of the tracking on 2 successive frames are demonstrated in Fig.2 and Fig.3 respectively. In all applications, time computing necessary is about 2mn on Sun Sparc10 for the complete procedure and the robust regression is the most computing demanding. In the future, it is planned to combine this approach with a tracking procedure based on Kalman filter techniques and to exploit a regularized optical flow field [17] to improve segmentation results and computational costs.

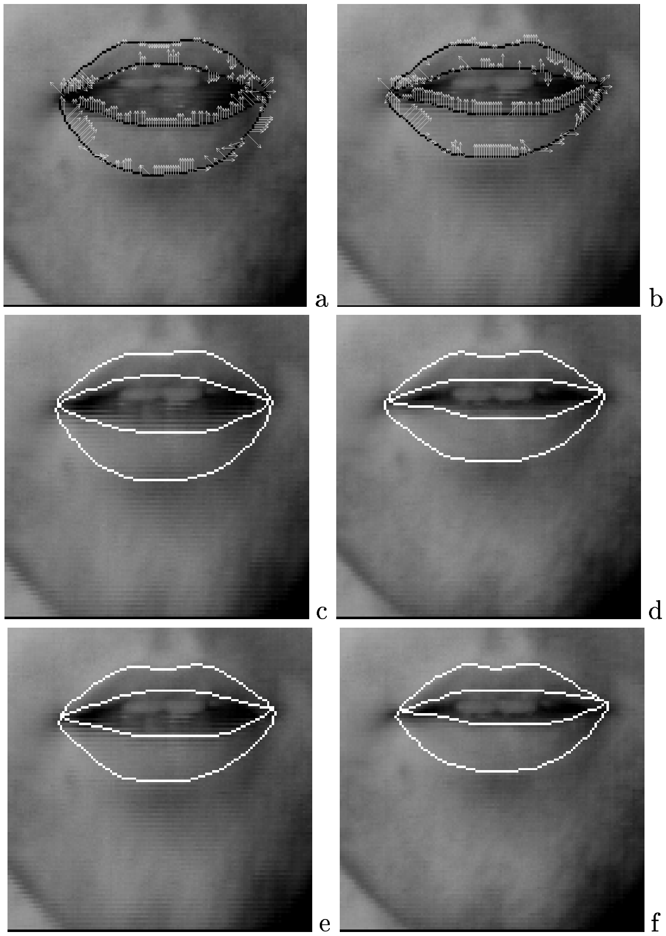

Figure 1: *Tracking of mouth movements*

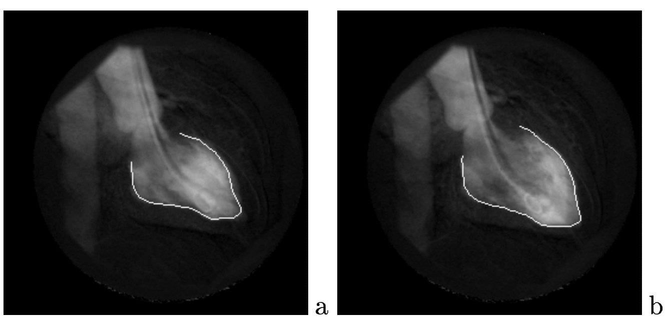

Figure 2: *Tracking of the ventricle in X-ray imagery.*

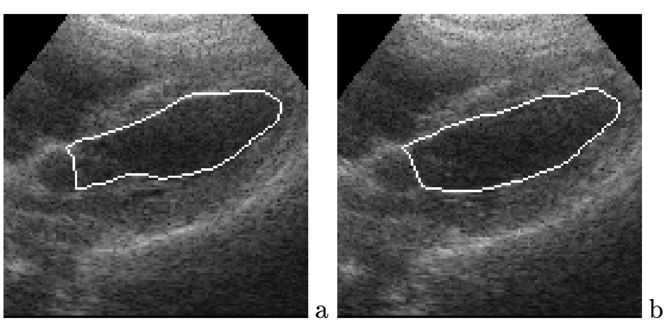

Figure 3: *Tracking of the ventricle in ultrasound imagery.*

References

[1] B. BASCLE, P. BOUTHEMY, N. DERICHE and F. MEYER. – Tracking complex primitives in an image sequence. – *In Proc. Int. Conf. on Pattern Recognition*, pages 426–431, Jerusalem, Israel, Oct. 1994.

[2] A. BAUMBERG and D. HOGG – Learning flexible models from image sequences. – In *In Proc. European Conference on Computer Vision*, pages 299–308, Stockolm, Sweden, May 1994.

[3] M.O. BERGER. – How to track efficiently piecewise curved contours with a view to reconstructing 3D objects. – *In Proc. 12th Int. Conf. on Pattern. Rec.*, pages 32–36, Jerusalem, Israel, Oct. 1994.

[4] M.J. BLACK, and Y. YACOOB. – Tracking and recognizing rigid and non-rigid facial motions using local parametric models of image motion. – *In Proc. Int. Conf. Comp. Vis.*, pages 374–381, Boston, USA, June 1995.

[5] A. BLAKE, R. CURWEN and A. ZISSERMAN. – A framework for spatiotemporal control in the tracking of visual contours. – *Int. J. Computer Vision*, Vol. 11, No 2: pp. 127–145, Oct. 1993.

[6] P. BOUTHEMY. – A maximum-likelihood framework for determining moving edges. – *IEEE Trans. Pattern Anal. Machine Intell.*, Vol. 11, No 5: pp. 499–511, May 1989.

[7] I. COHEN. – A nonlinear variational method for optical flow computation. – *In Proc. Scandinavian. Conf. Image Analysis*, pages 523–530, Tromso, Norway, May 1993.

[8] T. COOTES, C.J. TAYLOR, D.H. COOPER and J. GRAHAM. – Active shape models - Their training and application. – *CVGIP: Image Understanding*, Vol. 1, No 1, pages 38–59, 1994.

[9] R. CURWEN and A. BLAKE – Dynamic contours : real-time active splines. – *Active Vision*, MIT-Press, pages 39–57, 1992.

[10] I. ESSA and A. PENTLAND. – A vision system for observing and extracting facial action parameters. – In *In Proc. Comput. Vis. Pat. Rec.*, pages 76–83, Seattle, USA, June 1994.

[11] M. KASS and A. WITKIN and D. TERZOPOULOS. – Snakes: Active Contour Models. – *In Proc. Int. Conf. Comp. Vis.*, pages 259–268, London, UK, June 1987.

[12] C. KERVRANN and F. HEITZ. – A hierarchical Statistical Framework for the Segmentation of Deformable Objects in Image Sequences. – In *In Proc. Comput. Vis. Pat. Rec.*, pages 724–728 , Seattle, USA, June 1994.

[13] C. KERVRANN and F. HEITZ. – Robust tracking of stochastic deformable models in image sequences. – In *In Proc. Int. Conf. Image Processing*, Vol. 3, pages 88–92 , Austin, USA, Nov. 1994.

[14] C. KERVRANN and F. HEITZ. – Statistical model-based segmentation of deformable motion. – In *In Proc. Int. Conf. Image Processing*, Lausanne, Switzerland, Sept. 1996.

[15] A. MOHAMMAD-DJAFARI. – On the estimation of hyperparameters in bayesian approach of solving inverse problems. – *In Proc. Int. Conf. Acoust. Speech Signal Processing*, Minneapolis, USA, 1993.

[16] C. NASTAR and N. AYACHE. – Fast segmentation, tracking and analysis of deformable objects. – *In Proc. Int. Conf. Comp. Vis.*, pages 275–279, Berlin, Germany, May 1993.

[17] Y. RICQUEBOURG and P. BOUTHEMY. – A statistical regularization framework for estimating normal displacements along contours with subpixel accuracy. – *In Proc. Comp. Anal. of Images and Patterns*, Prague, Czech Republic, Sept. 1995.

[18] P.J. ROUSSEEUW and A.M. LEROY. – Robust regression and outliers detection – *John Wiley and Sons*, 1987.

[19] K.Y. WOHN, J. WU and R.W. BROCKETT. – A contour-based recovery of image flow: iterative transfromation method. – *IEEE Trans. Pattern Anal. Machine Intell.*, Vol. 13, No 8: pp. 746–760, Aug. 1991.

[20] A. YUILLE, P. HALLINAN and D. COHEN. – Feature extraction from faces using deformable templates. – *Int. Journal of Comput. Vis.*, Vol. 8, No 2: pp. 99–111, 1991.